METALS AND MATERIALS, Vol. 4, No. 3 (1998), pp. 566~572

Molecular Dynamics Simulation on Dislocation Emission Process

Tzuchiang Wang and Qiheng Tang

LNM, Institute of Mechanics, Chinese Academy of Sciences, Beijing 100080, China

A correlative reference model for a computer simulation of molecular dynamics is proposed in this paper. Based on this model, a flexible displacement boundary scheme is naturally introduced and the dislocations emitted from a crack tip are presumed to continuously pass through the border of an inner discrete atomic region to pile up at an outer continuum region. The simulations for a Mo crystal show that the interaction between a crack and emitted dislocations results in the decrease in local stress intensity factor gradually.

Key words : correlative reference model, molecular dynamics, dislocation emission, flexible displacement boundary scheme, dislocation velocity

1. INTRODUCTION

Rice and Thomson [1] proposed a criterion for dislocation emission from a stressed crack tip, which is quite simple and can be applied to intrinsically brittle and ductile materials. Sinclair and Finnis [2] extended the Rice and Thomson analysis to address the problem of whether the presence of one or more emitted dislocations affects the competition between further emission and cleavage. Lin and Hirth [3] studied the stress changes with dislocations nucleated from a crack. Rice [4] used the Peierls concept to reanalyze the dislocation nucleation from a crack tip and proposed a new solid state parameter γ_{us}, the unstable stacking energy, to evaluate the critical external loading which corresponds to dislocation nucleation. Wang [5] extended Rice's analysis with a set of new governing equations to analyze the dislocation emission.

The above analyses were unsatisfactory to determine the near crack tip fields due to that they used the continuum elasticity for a crack tip stress field. Near the crack tip region, the atomic lattice effect becomes important and therefore an atomic force law needs to be considered.

Using the embedded atom method (EAM), Baskes *et al.* [6] investigated dislocation mobility in nickle. Applying a 3-dimensional MD method, to a crystal Cu, Zhang *et al.* [7] simulated dislocation emission and its mechanical behavior near a crack tip to obtain a series of interesting results with a fixed displacement boundary condition.

As pointed out by Cheung *et al.* [8], a proper choice of boundary condition on the border of inner discrete atomic region is of crucial importance for the accuracy of final results. Generally speaking, there are three types of boundary schemes in a MD simulation, a fixed displacement boundary scheme, a flexible displacement displacement boundary scheme, and a force (stress) boundary scheme. The fixed displacement boundary condition has been used by many authors [9]. The positions of atoms on the border are given according to linear elasticity theory and subsequently held fixed as the outer materials are removed during a simulation. Incompatibilities between the inner discrete atomic region and outer continuum region will arise at the border unless a flexible displacement boundary scheme is employed. Various versions of flexible displacement boundary scheme have been proposed [10]. In this case, the atoms forming the border of an inner system are given appropriate positions characteristic of the outer region. As the discrete interior region, still attached to the outer continuum, relaxes during a simulation, forces are generated on atoms located in a border region. These forces are then relieved in an iterative fashion through the use of a Green' s function derived from a linear elasticity theory. The third type of boundary scheme is to use a set of forces (or stresses) prescribed along the border of a discrete atomic region. These forces are obtained from an appropriate linear elasticity solution. The outer region is then removed while the forces on the border atoms are maintained throughout a simulation.

A particularly serious deficiency can arise from both the fixed boundary and flexible boundary conditions with the use of a Green's function due to its inability of

admitting dislocations to pass through the border. The force boundary condition offers no resistance to the penetration of dislocations through the border into an outer region, but it gives dynamically too complex results to describe the essence of a fracture process [11]. The size of a crystal area modeled in a atomic level computer simulation study is restricted to the order of ten or hundred thousand atoms by computer cost. Often this is too small for an atomic level simulation to reveal the complex properties of materials.

A correlative reference model is proposed in this paper. Based on this model, a new flexible displacement boundary scheme for an atomic level computer simulation is developed which provides several advantages over the previous boundary schemes:

(1) It offers no resistance for emitted dislocations to penetrate through the border.

(2) It eliminates an instability problem encountered with the specified force boundary method.

2. MECHANICAL MODEL

The correlative reference model is schematically shown for a simulated sample of MD approach with a single edge crack in Fig. 1a. The region 1 in the figure contains inner discrete atoms, while the region 2 represents the border of inner simulated atoms. S_R represents an emitted dislocation. Fig. 1b shows an infinite continuum containing a single edge crack with its elastic constants, such as E, G, and ν, being the same as those of a simulated Mo crystal. The geometric configuration and the size outlined by the dotted line in Fig. 1b are also the same as those given in Fig. 1a. This infinite elastic continuum is designated as a reference model subjected to a remote loading. There is a certain correlation between a simulated real sample and the reference model. Two requirements must be satisfied in the simulation.

(1) The displacements of atoms in the region 2 in Fig. 1a is imposed by the displacements of coresponding region in a reference model.

(2) With N_T dislocations emitted from a crack tip, here $N_T=N_1+N_3$, the positions of N_1 emitted dislocations in the region 1 of Fig. 1b are defined by the discrete atomic configuration in Fig. 1a, while the positions of remaining N_3 dislocations in the continuum region 3 are determined by the dislocation pileup theory of micromechanics.

2.1. Simulation procedure

2.1.1. Flexible displacement

Consider first the problem of the reference model, the

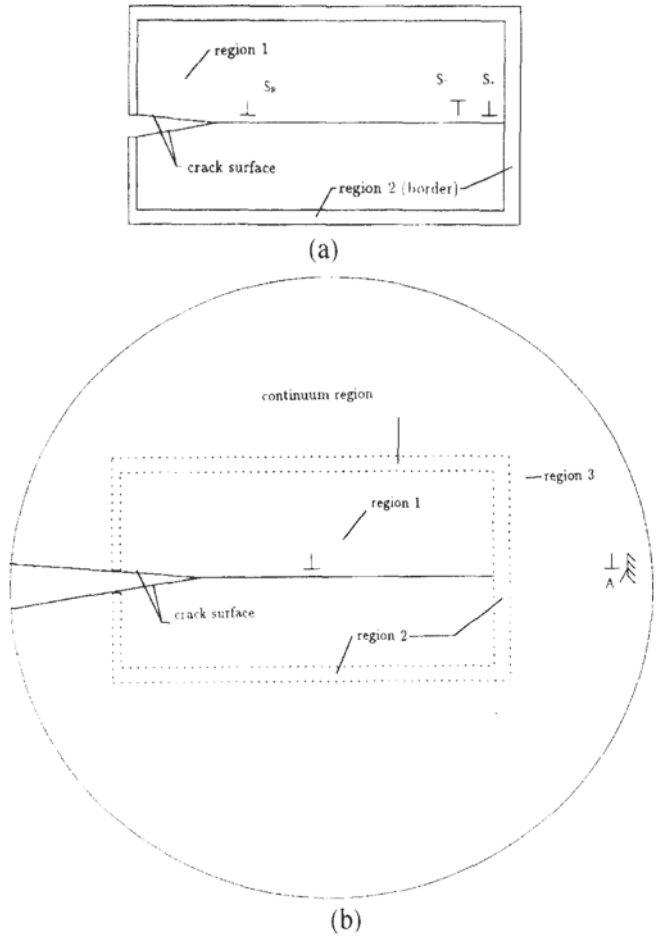

Fig. 1. Schematic diagram for the correlative reference model. (a) Schematic diagram for the simulated sample, (b) Schematic diagram for the infinite continuum with a single edge crack

pure K_{II} stress field is prescribed at infinity with the stress intensity factor K_{II} taken as a load parameter. The slip plane is taken to coincide with the crack plane with the slip direction paralled to the x axis in the present study. Hence all emitted dislocations lie on the x axis. The displacement field of an infinite continuum with a single edge crack and N_T discrete dislocations can be obtained from a linear elasticity theory as,

$$u_l = u_l^A + \sum_{i=1}^{N_T} u_l^D(x, y; x_i) \tag{1}$$

where the subscript l denoting the usual coordinate components of x and y directions, x_i the position of the *i-th* discrete dislocation, u_l^A and u_l^D the displacement fields due to an applied remote loading and dislocations, respectively. The displacement u_l depends not only on the applied remote load but also on the emitted dislocations.

Before any dislocation emission, the displacement field in the reference model is just pure K_{II} field and the displacements imposed on the atoms in the border of discrete atomic system are also pure K_{II} field. Hence the present boundary condition is actually the same as the fixed displacement boundary condition until a first dislocation is nucleated.

When a dislocation is nucleated in a crack tip region, which can be detected from a MD simulation on a discrete atomic system in Fig. 1a, we will pause to load temporarily and to keep the remote load K_{II} unchanged in the reference model. The displacements of atoms on the border in Fig. 1a, which are given by the displacements of the region 2 of the reference model, are held fixed temporarily and then the discrete atom system is relaxed.

Because of the unstable characteristics of emitted dislocations near the crack tip, it is impossible for a nucleated dislocation to stay at a crack tip and consequently the dislocation S_R moves away from the crack tip. Although the external load at infinity is held fixed, the displacement fields will vary with a dislocation emission or glide which provides displacement increment to the reference model. The displacement field imposed on the border of discrete atom system in Fig. 1a is also changed during the relaxation process of MD simulation. Therefore the present boundary condition prescribed on the border of MD simulated sample is essentially a flexible displacement boundary condition. The emitted dislocations will pass through the border. If there are still some dislocations in the discrete atom region 1, relaxation will be carried on continuously; Otherwise, we will load at infinity again with the same loading rate as before in the reference model.

2.1.2. Dislocation penetration

Numerous experimental observations have shown that dislocations are emitted from a stressed crack tip when an applied stress intensity factor is greater than K_{IIe}, and thet dislocations can be emitted continuously when the applied load increases slightly. The emitted dislocations are also observed to glide along the slip plane and to pile up eventually against strong obstacles such as a grain boundary or other impuries at the distance of several micrometers from a crack tip.

In our simulation, the first emitted dislocation is assumed to pile up at point A, located at the distance of $5000a_0$ from the crack tip, far beyond the relatively small size of the present sample. A satisfactory result can not be obtained unless the emitted dislocations can penetrate through the border into the continuum region smoothly. It is assumed that both the positive and negative dislocations, marked by S_+ and S_- respectively, can be located near the border. As the emitted dislocation S_R glides to the border to interact with dislocation S_-, dislocations S_R and S_- will be annihilated leaving only the dislocation S_+ near the border. Its velocity is the same as that of the emitted dislocation S_R, because it is replaced by dislocation S_+ in the region 1. Moreover as S_+ penetrates through the border, its velocity should be evaluated reasonably based on the velocity of the emitted dislocation. Because the border is no longer an obstacle to affect dislocation motion, the width of the border is very narrow and the velocity of the emitted dislocation S_R is nearly constant beyond the distance of $5a_0$ from a crack tip. The velocity of dislocation S_+ is regarded practically the same as the velocity of emitted dislocation in our simulation. When the dislocation S_+ passed through the border into the region 3, a step has been formed on the right border. After that the glide effect of emitted dislocation S_+ on the positions of the atoms in the border becomes much smaller.

2.1.3. Positions in region 3

The positions of N_3 emitted dislocations in the region 3 of Fig. 1b can be determined by the following equations:

$$\begin{cases} x_1 = x_{Ob} \\ \tau_i = \tau_f, \ i = 2, 3, ..., N_3 \end{cases} \tag{2a}$$

$$\tau_i = \frac{K_{II}}{\sqrt{2\pi x_i}} + \frac{2Gb}{(\kappa+1)\pi}\left[-\frac{1}{2x_i} + \sum_{j=1,\, j\neq i} \frac{\sqrt{x_j}}{\sqrt{x_i}\,(x_i - x_j)}\right] \tag{2b}$$

where x_{Ob} and x_i are the first and the *i-th* dislocation positions respectively, τ_i is the shear stress acting on the *i-th* dislocation including the K_{II} field produced by the external loading, its own image stress and the stress of all other emitted dislocations both in the region 1 and region 3 and their images. G denotes the shear modulus, b the Burgers vector, and τ_f the lattice friction stress.

It should be noted that all emitted dislocations lie on the x-axis. The dislocation number is counted from the right to left so that, the dislocation positions are x_i (i=1, 2, ..., N_3) in the region 3 and x_i (i=N_3+1, ..., N_T) in the region 1, respectively.

In the reference model, any movement of dislocations in the region 1 should affect the distribution of emitted dislocations in region 3. And the change of dislocation positions in region 3 will conversely provide the displacement increment to the reference model. If this simulation were carried out in such a way, the non-linear Eq. 2 would be solved per time step and computational cost

would be increased sharply. The emitted dislocations in region 3 pile up in a plastic zone which is far away from the crack tip, hence the redistribution effect of emitted dislocations in a plastic zone on the displacement of region 1 can be regarded as quite small. In order to reduce the computation cost, a simple method is adopted in our simulation. As the nucleated dislocations move within region 1, the positions of N_3 dislocations in region 3 were held fixed temporarily. But as the (N_3+1)-*th* dislocation penetrates through the boundary into the region 3, the Eq. 2 are solved by the Newton-Raphson method and, the dislocation positions in region 3 will be redistributed. The effect of dislocation position redistribution in region 3 is accounted for in our simulation.

2. BASIC FORMULAS

The displacement field u_i^A of Eq. 1 is given by the linear elastic fracture theory as,

$$\begin{cases} u_x^A = \dfrac{K_{II}}{4G}\sqrt{\dfrac{r}{2\pi}}\left[(2\kappa+3)\sin\dfrac{\theta}{2}+\sin\dfrac{\theta}{3}\right] \\ u_y^A = \dfrac{K_{II}}{4G}\sqrt{\dfrac{r}{2\pi}}\left[(2\kappa+3)\cos\dfrac{\theta}{2}+\cos\dfrac{\theta}{3}\right] \end{cases} \tag{3}$$

where r is the distance from the crack tip, $\kappa=(3-4\nu)$ with ν denoting the Poisson's ratio. The displacement field u_i^D is given by,

$$2G(u_x^D+iu_y^D) = \kappa\phi(z)-\omega(\bar{z})-(z-\bar{z})\overline{\Phi(z)} \tag{4}$$

According to Lo [12], the complex functions $\Phi(z)$, $\Omega(z)$, $\phi(z)$ and $\omega(z)$ can be expressed as

$$\Phi(z)=\Omega(z)=\Phi_0(z)+\Phi_R(z)=\frac{B}{z-z_0}\sqrt{\frac{z_0}{z}} \tag{5a}$$

$$\phi(z)=\omega(z)=\int\Phi(z)dz=B\ln\frac{\sqrt{z}-\sqrt{z_0}}{\sqrt{z}+\sqrt{z_0}} \tag{5b}$$

where $B=\dfrac{bG}{(\kappa+1)\pi i}$. If the emitted dislocation lies on the x axis, at $z_0=x_0$, the displacement field u_i^D can be represented as

$$u_x^D+iu_y^D=\frac{b}{2i\pi(\kappa+1)}\left[\kappa\ln\frac{\sqrt{z}-\sqrt{x_0}}{\sqrt{z}+\sqrt{x_0}}-\ln\frac{\sqrt{\bar{z}}-\sqrt{x_0}}{\sqrt{\bar{z}}+\sqrt{x_0}}-(z-\bar{z})\frac{1}{z-x_0}\sqrt{\frac{x_0}{z}}\right] \tag{6}$$

3. CALCULATION METHOD

3.1. Interatomic potential

The 'N-body' potential has been proposed by Tang *et al.* [13] in which the embedded energy function was obtained by means of a numerical experiment for uniaxial tension. The total energy E_T of an assembly of atoms is

$$E_T=\frac{1}{2}\sum_{i,j\,i\neq j}\phi(r_{ij})+\sum_i F\left(\frac{\rho_i}{\rho_e}\right) \tag{7}$$

where r_{ij} is the distance between atoms i and j, $\phi(r_{ij})$ is the pair-potential, $F(\rho_i/\rho_e)$ is the embedded energy function. For a Mo crystal, the functions of $\phi(r_{ij})$ and $F'(\rho_i/\rho_e)$ can be expressed by following equations [13].

$$\begin{aligned}\phi\left(\frac{r_{ij}}{r_{1e}}\right) &= B_0+B_1\left(\frac{r_{ij}}{r_{1e}}-1\right)+B_2\left(\frac{r_{ij}}{r_{1e}}-1\right)^2+B_3\left(\frac{r_{ij}}{r_{1e}}-1\right)^3 \\ &\quad +H(r_{ij}-r_{2e})\left[B_4\left(\frac{r_{ij}}{r_{1e}}-1\right)^3+B_5\left(\frac{r_{ij}}{r_{1e}}-1\right)^3\right. \\ &\quad \left.\left(\frac{r_c}{r_{2e}}-1\right)\right]\Big/\left(\frac{r_c}{r_{2e}}-1\right)^3\end{aligned} \tag{8}$$

$$F'\left(\frac{\rho}{\rho_e}\right) = \begin{cases} -10\sqrt{0.0515-(\dfrac{\rho}{\rho_r}-0.778)^2}+1.9, & 0.68\le\dfrac{\rho}{\rho_e}\le 0.775 \\ -0.72(\dfrac{\rho}{\rho_e}-0.775)6-0.3, & 0.775\le\dfrac{\rho}{\rho_e}\le 0.83 \\ -10\sqrt{0.397-(\dfrac{\rho}{\rho_e}-0.88)^2}+0.59, & 0.83\le\dfrac{\rho}{\rho_e}\le 1.01 \end{cases} \tag{9}$$

where ρ_i is the atomic electron density, r_{1e} and r_{2e} are the first- and second- neighbor atom distance, respectively. The coefficients B_i, $(i=1, \ldots, 6)$ in the Eq. 8 were given in the paper [13]. $H(r_{ij}-r_{2e})$ is a step function, ρ_e is the equilibrium atomic electron density.

3.2. Atomic lattice geometry

The parallelopiped with a slit is used as the simulated sample in the present calculation. The coordinate system is selected to be x, y and z axes along [111], [1$\bar{1}$0], and [11$\bar{2}$], respectively as depicted in Fig. 2. The lengths of x, y and z are $500\times\dfrac{\sqrt{3}}{6}a_0$, $40\times\dfrac{\sqrt{2}}{2}a_0$ and $6\times\dfrac{\sqrt{6}}{6}a_0$, respectively. The left side of boundary is located at $120\times\dfrac{\sqrt{3}}{6}a_0$ from the crack tip, while the separation of the upper and lower crack planes is taken to be $\sqrt{2}a_0$. The total number of atoms in the present simulation is about 20000.

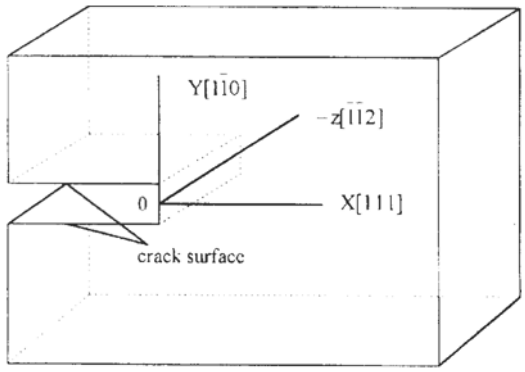

Fig. 2. Schematic diagram for the simulated sample.

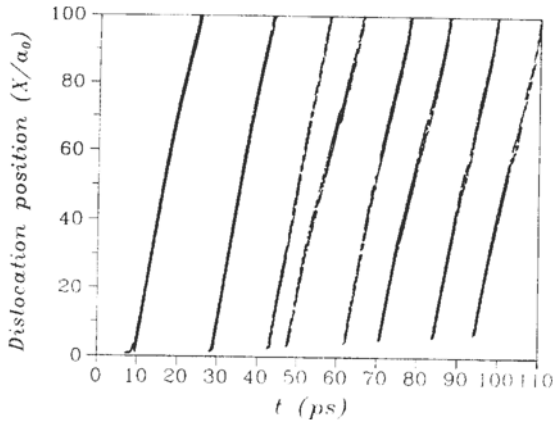

Fig. 3. Distance of dislocation position from crack tip plotted versus time.

3.3. Calculation method

The leapfrog algorithm [14] is used in this paper, the loading rate of K_{II} =0.0706(MPam$^{1/2}$/ps). The stress intensity factor K_{II} is chosen as the loading parameter. The time step is 1.256×10^{-14}s.

3.4. Temperature condition

The initial velocity of atoms is taken to have the Maxwellian distribution corresponding to a given temperature. The simulated system is supposed to be connected to a big heat source with a certain temperature providing an enough heat energy to maintain the system at a fixed temperature, here T=50 K, throughout the duration of the runs. This means that any a little perturbation due to a continuous loading or dislocation emission can be neglected [14].

4. RESULTS AND DISCUSSION

The positions of the eight fully emitted dislocations are plotted as a funotion of time in Fig. 3. The eight perfect dislocations (24 partial dislocations) glide into region 3 smoothly and are assumed to pile up at the distance of $5000a_0$ from the crack tip. The simulated results of MD show that a perfect dislocation is dissociated into three partial dislocations in a bcc Mo crystal, but two partial dislocations in a fcc Cu crystal [7]. Additionally the extensive distance among the three partial dislocations of Mo is found much shorter than that of Cu with the values of about $4a_0$ and $20a_0$, respectively.

When the first three partial dislocations are emitted, the load is temporarily paused and keeping the load unchanged in the reference model. The nucleated dislocation is then subjected to a repulsive force from the K_{II} external stress field and gliding away on the slip plane with a high velocity. The dislocation is in an accelerative state within the distance of $5a_0$ from the crack tip, and then reaches a constant velocity state quickly. Within the distance of between $5a_0$ and $100a_0$, all the eight dislocations are almost at the same velocity within the range about of 1800 m/s to 1950 m/s, which is less than the shear wave velocity of about 3500 m/s for a Mo crystal.

In a time scale of ps or fs, the time interval of dislocation emission is not homogeneous with, the longest time interval of 20ps between the first and the second emission, while the shortest is 6ps between the third and the fourth.

The dislocation emission is, however, regarded as, continuous in a time scale of μs or ms. The simulated result is in a good agreement with the experiment observation [15].

As the emitted dislocations glide away from the crack tip, the interaction between the dislocation and crack becomes very small, so that the interaction among dislocations becomes predominaht at this stage. The result shows that the space interval between the third and fourth dislocations is from narrow to wider gradually.

In our simulation the first three partial dislocations sliped into the region 3 at t=29ps. Because no other dislocation is found in the region 1, the load is again increased at the same loading rate as before. As K_{II} reaches at 0.801 MPa$\sqrt{m}$, the second perfect dislocation is emitted. Compared with the critical stress intensity factor K_{IIe}=0.668MPa$\sqrt{m}$ of the first perfect dislocation emission, the loading increment is about 10% of K_{IIe}. The loading increment is less than 1% of the K_{IIe} from the third to the eighth pertect dislocation. The dislocation distance from the crack tip is depicted in terms of the external stress intensity factor K_{II} in Fig. 4.

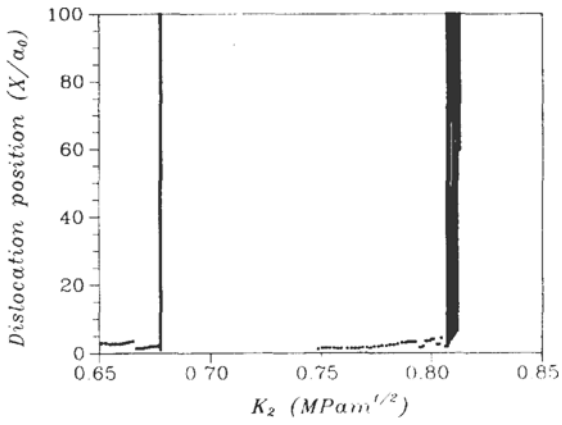

Fig. 4. Distance of dislocation position from crack tip plotted against stress intensity factor.

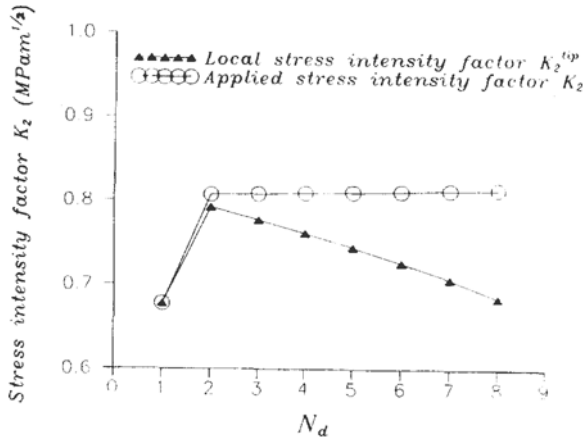

Fig. 5. External stress intensity factor compared to the local stress intensity factor, the stress intensity factor versus dislocation number is plotted.

According to Rice [1], the interaction between the dislocation and crack leads to the decrease in a local stress intensity factor K_{II}^{tip} after the dislocation emitted from the crack tip, which is given by,

$$K_{II}^{tip} = K_{II} - 2\sqrt{2\pi}Ab\sum_{i=1}^{n}\frac{1}{\sqrt{x_i}}. \quad (13)$$

The result in Fig. 4 shows that the second perfect dislocation is emitted at K_{II}=0.80 MPa $m^{1/2}$, corresponding to an external loading increment of up to approximately 10% of K_{IIe}. The external loading increment is, however, quite smaller for in the following dislocation emissions. There may be two factors affecting the differences in loading amount between the first and the second dislocation emission. Firstly, deformation near crack tip region is still in a stable state after the first dislocation piles up at the distance of $5000a_0$ from the crack tip at the external load of K_{II}=0.668 $MPam^{1/2}$. No evidence for a nucleation of next dislocation near the crack tip is observed within the subseguent relaxation of 100 time step, unless reloading is carried out again at infinity in the reference model. As the external load reaches K_{II}=0.801 $MPam^{1/2}$, deformation in the discrete atom region becomes, however, an unstable state to emit more than two perfect dislocations continuously. The other is that the reloading rate is too high after the first dislocation glides into the region 3 leading into such a difference of loading amount.

Based on Eq. 13, the local stress intensity factor K_{II}^{tip} can be obtained to show a gradual decrease as given in Fig. 5. Suggesting that the local stress intensity factor may not be a proper control parameter in the study of a crack tip dislocation emission.

5. CONCLUSIONS

(1). Both the correlative reference model and the flexible displacement boundary model have been presented which offer several advantages over the previous schemes. The problem of dislocation penetration through the border has been solved successfully. Although the size of simulated atomistic core is finite, the number of emitred dislocations can increase without restrictions.

(2) The molecular dynamics simulation for a Mo crystal, shows that dislocations can be emitted from the crack tip continuously with increase in applied load after the second dislocation is emitted.

(3) Within the distance of $5a_0$ from the crack tip, the dislocation is in an accelerative state and reaches the stable velocity quickly, while the dislocation velocity is nearly constant having the value of about 1800 m/s-1950 m/s within the range of between $5a_0$ and $100a_0$, which is in an agreement with that predicted previously [18].

ACKNOWLEDGEMENTS

The research work presented here was supported by the National Natural Science Foundation of China (No. 19704100) and the National Sciences Foundation of Chinese Academy of Sciences (project KJ 951-1-201).

REFERENCES

1. J. R. and Rice, R. Thomson, *Phil. Mag.* **29**, 73 (1974).
2. J. E. Sinclair and M. W. Finnis, in *Atomics of Fracture* (eds., R. M. Latanision, J. R. Piokens), Plenum press (1983).
3. I. H. Lin and J. P. Hirth, *Phil. Mag.* **A50**, L43 (1984).
4. J. R. Rice, *J. Mech. Phys. Solids* **40**, 239 (1992).

5. T. C. Wang, *Int. J. Fract.* **69**, 295 (1995).
6. M. I. Baskes, M. S. Daw and S. M. Foiles, *Mater. Res. Soc. Symp. Proc.* **141**, 31 (1989).
7. Y. W. Zhang, T. C. Wang and Q. H. Tang, *J. Appl. Phys.* **77**, 2393 (1995).
8. K. S. Cheung, A. S. Argon and A. S. Yip, *J Appl. Phys.* **69**, 2088 (1991).
9. P. C. Gehlen and M. F. Kanninen, *Inelastic Behavior of Solids* (eds., M. F. Kanninen, W. F. Alder, A. R. Rosenfield and R. I. Jaffee), p. 587, McGraw-Hill, New York (1970).
10. J. E. Sinclair, *J. Appl. Phys.* **42**, 5321 (1971).
11. H. Kitagawa and A. Nakatani, *Proceeding if JSMED Ser.* **A59**, 256 (1993).
12. K. K. Lo, *J. Appl. Mech.* **45**, 797 (1978).
13. Q. H. Tang, T. C. Wang and Y. W. Zhang, *Acta Mech. Sinica* **4**, 358 (1996).
14. D. W. Heermann, *Computer simulation methods in theoretic physics*, 2nd Edition, Springer-Verlag, Berlin (1990).
15. J. A. Horton and S. M. Ohr, *J. Mater. Sci.* **17**, 3140 (1982).
16. I. Alber, J. L. Bassani, Specify all the sames. *Phil. Trans. R. Soc. Lond. A* **339**, 555 (1992).
17. R. E. Peierls, *Proc. Phys. Soc.* **52**, 34 (1940).
18. J. J. Gilman, *J. Appl. Phys.* **31**, 2208 (1960).